

Research Article

Some New Soliton Solutions of Time Fractional Resonant Davey–Stewartson Equations

Esin İlhan ¹, Muhammed Yiğider ², Ercan Çelik ^{3,4} and Hasan Bulut ^{5,6}

¹Faculty of Engineering and Architecture, Kırşehir Ahi Evran University, Kırşehir, Türkiye

²Department of Mathematics, Erzurum Technical University, Erzurum, Türkiye

³Department of Applied Mathematics and Informatics, Kyrgyz-Turkish Manas University, Bishkek, Kyrgyzstan

⁴Department of Mathematics, University of Ataturk, Erzurum, Türkiye

⁵Department of Mathematics, University of Fırat, Elazığ, Türkiye

⁶Azerbaijan University, Baku, Azerbaijan

Correspondence should be addressed to Ercan Çelik; ercan.celik@manas.edu.kg

Received 30 July 2024; Accepted 26 February 2025

Academic Editor: Rajesh Kumar

Copyright © 2025 Esin İlhan et al. Computational and Mathematical Methods published by John Wiley & Sons Ltd. This is an open access article under the terms of the Creative Commons Attribution License, which permits use, distribution and reproduction in any medium, provided the original work is properly cited.

In this study, the Bernoulli subequation method (BS-EM) is applied to investigate the traveling wave solutions of the $(2 + 1)$ -dimensional resonant Davey–Stewartson system. By employing a wave transformation, the system's nonlinear partial differential equation is reduced to a nonlinear ordinary differential equation, which is then solved using the BS-EM approach. As a result, several new traveling wave solutions, which have not been previously reported in the literature, have been successfully obtained. These solutions provide new insights into the physical dynamics of the system and also satisfy the $(2 + 1)$ -dimensional time–fractional resonant Davey–Stewartson equation. Furthermore, the analytical and graphical analyses of the obtained solutions have been carried out, and the wave profiles have been examined under various parameter conditions. All computations and graphical visualizations in this study were performed using the Wolfram Mathematica 12 software.

Keywords: resonant Davey–Stewartson equation; the Bernoulli subequation method (BS-EM); the fractional Riemann–Liouville derivative

1. Introduction

Many fields of study, such as physics, mechanics, and material science, use nonlinear evolution equations (NLEEs). The search for solitary wave solutions plays a very important fundamental role in the NLEEs since they describe numerous features of our real-life situations. New research shows the importance and status of the development of soliton types in differential systems [1, 2]. Numerous methods for obtaining the analytical solutions of different types of partial differential equations (PDEs) have been explored. PDEs attract such as simplified Hirota's method [3], $(m + G'/G)$ –expansion method [4], the Bernoulli sub-ODE method [5, 6], symbolic computational method [5–8], multiple Exp-function method

[9, 10], the generalized exponential rational function method [11, 12], and many other methods [13–15].

In the literature, researchers have utilized a variety of approaches to find specific types of solutions, such as accurate, numerical solutions. Zhao et al. studied the Davey–Stewartson equation and obtained one and two soliton solutions [16], Tang et al. have applied with the help of the Painlevé test to DS equations [17–19], and by many researches, other methods have been applied to investigate which soliton wave solutions of the resonant Davey–Stewartson equation system will yield [20–23].

This paper has five parts in its most general form: In the second section, general definitions about the overview of conformable fractional derivatives are given. The third sec-

tion is the application steps of the Bernoulli subequation method. In Section 4, resonant Davey–Stewartson equations [24] and its application will be introduced and expressed in more detail. In Section 5, evaluations were written with the result section, and in the last section, discussion was given place.

2. Overview of Conformable Fractional Derivatives

Here, some basic definitions, properties, and theorems about conformable fractional derivatives are discussed [25–27]. Recently, new fractional calculus operators like as the Caputo Fabrizio, the Riemann Liouville, and the Beta derivative have been used to study the characteristics of fractional PDEs. These kinds of models are crucial to solving difficult models in the applied sciences and engineering domains. The conformable fractional derivative is one of these models that helps us understand the nature of the model.

Definition 1. ($R-L$ and $C-F$) A real function $z(t)$, $t > 0$ is said to be in space C_ν ; $\nu \in \mathbb{R}$ if there exists a real number $k(>\nu)$, such that $u(t) = t^k u_1$, where $u_1(t) \in C[0, \infty)$ which is also in space C'_ν if and only if $u^{(n)} \in C_\nu$, $n \in \mathbb{N}$.

$${}^{RL}D_{0,t}^\alpha u(t) = \frac{1}{\Gamma(n-\alpha)} \frac{d^n}{dt^n} \int_0^t (t-\xi)^{n-\alpha-1} u(\xi) d\xi \quad (1)$$

$${}^CD_{0,t}^\alpha u(t) = \frac{1}{\Gamma(n-\alpha)} \int_0^t (t-\xi)^{n-\alpha-1} \frac{d^n}{dt^n} u(\xi) d\xi \quad (2)$$

$n-1 < \alpha \leq n$

Definition 2. (Beta-derivative) Take f be a function such that

$$f: [\alpha, \infty) \rightarrow \mathbb{R}$$

$${}^AD^\beta(f(x)) = \lim_{\varepsilon \rightarrow 0} \frac{f\left(x + \xi(x + 1/\Gamma(\beta))^{1-\beta}\right) - f(x)}{\varepsilon} \quad (3)$$

$x \geq \alpha, \beta \in (0, 1]$

Definition 3. Let $g: (0, \infty) \rightarrow \mathbb{R}$; then, the conformable fraction derivative of g of order α is defined as

$$T_\alpha(g)(t) = \lim_{\varepsilon \rightarrow 0} \frac{g(t + \varepsilon t^{1-\alpha}) - g(t)}{\varepsilon}, t > 0, 0 < \alpha < 1 \quad (4)$$

Here, some basic properties of conformable fractional derivatives [24] are presented.

$$T_\alpha(bg + ch) = bT_\alpha(g) + cT_\alpha(h), b, c \in \mathbb{R} \quad (5)$$

$$T_\alpha(t^x) = xt^{x-\alpha}, x \in \mathbb{R} \quad (6)$$

$$T_\alpha(gh) = gT_\alpha(h) + hT_\alpha(g) \quad (7)$$

$$T_\alpha\left(\frac{g}{h}\right) = \frac{hT_\alpha(g) - gT_\alpha(h)}{h^2} \quad (8)$$

$$\text{If } g \text{ is differentiable, then } T_\alpha(g)(t) = t^{1-\alpha} \frac{dg}{dt} \quad (9)$$

The chain rule and other significant features are obeyed by the conformable differential operator.

Theorem 1. Assume that $g_2(x, t)$ is differentiable and well-defined throughout the range of $g_1(x, t)$, and that $g_1(x, t)$ is a α -conformable differentiable function

$$T_t^\alpha(g_1(t) \circ g_2(t)) = t^{1-\alpha} \frac{dg_2}{dt} \frac{d}{dt}(g_1(g_2(t))) \quad (10)$$

3. General Forms of the Bernoulli Subequation Method

In this step, we have expressed the implementation steps of BSEM:

Step 1: Let us consider the equation, the most general form of which is given as Equation (11), as follows:

$$P(u_x, u_t, u_{xt}, u_{xx}, \dots) = 0 \quad (11)$$

$$\phi(x, y, t) = e^\theta U(\eta), \quad \varphi(x, y, t) = V(\eta)$$

$$\theta = i\mu \left(x + y - c \frac{t^\alpha}{\Gamma(\alpha+1)} \right), \quad \eta = \alpha x + \beta y + \gamma \frac{t^\alpha}{\Gamma(\alpha+1)} \quad (12)$$

where $\gamma \neq 0$. With the help of the wave transform given in Equation (12), the ordinary differential equation given in Equation (3) can be obtained.

$$N(U, U', U'', \dots) = 0 \quad (13)$$

Step 2: In the case of Equation (13), the trial equation of solution can be stated as follows:

$$U(\eta) = \sum_{i=1}^n a_i F^i = a_0 + a_1 F + a_2 F^2 + \dots + a_n F^n \quad (14)$$

$$F' = bF + dF^M, b \neq 0, d \neq 0, M \in \mathbb{R} - \{0, 1, 2\} \quad (15)$$

Here, $F(\eta)$ symbolize the Bernoulli differential polynomial. Equation (14) and Equation (15) are emplaced into Equation (13), and we get a polynomial $\Omega(F(\eta))$ of $F(\eta)$ as follows:

$$\Omega(F(\eta)) = \rho_s F(\eta)^s + \dots + \rho_1 F(\eta) + \rho_0 = 0 \quad (16)$$

Due to the principle of balance, we find the relation between n and M .

Step 3: Assuming that the coefficients of $\Omega(F(\eta))$ all be zero, the resulting is an algebraic system of equations:

$$\rho_i = 0, i = 0, \dots, s \quad (17)$$

Solving Equation (17), we evaluate the values a_0, \dots, a_n .

Step 4: Solving the Bernoulli differential equation for Equation (14), we get two solutions due to b and d :

$$F(\eta) = \left[\frac{-d}{b} + \frac{E}{e^{b(M-1)\eta}} \right]^{1/1-M}, b \neq d \tag{18}$$

$$F(\eta) = \left[\frac{(E-1) + (E+1) \tan(b(1-M)\eta/2)}{1 - \tan(b(1-M)\eta/2)} \right]^{1/1-M} \tag{19}$$

$b = d, E \in \mathbb{R}$, where $E \neq 0$ is integration constant. Utilizing Wolfram Mathematica software, we obtain the solutions to Equation (13). Giving the proper parameter values to the obtained wave solutions allows three-dimensional wave graphs to be drawn.

4. The (2 + 1)-Dimensional Davey–Stewartson Equations and Implement of BSE Method

In this part of the work, the (2 + 1)-dimensional Davey–Stewartson equations [24] are considered

$$u_t^\alpha + \sigma^2 u_{xx} + u_{yy} - 2\sigma^2 \left(\frac{|u|_{xx}}{|u|} + \sigma^2 \frac{|u|_{yy}}{|u|} \right) u - \nu u + \omega |u|^2 u = 0 \tag{20}$$

$$v_{xx} - \sigma^2 v_{yy} - 2\omega (|u|^2)_{xx} = 0 \tag{21}$$

The amplitude of a surface wave packet is represented by $u(x, y)$, the velocity potential of the mean flow interacting with the surface wave is represented by $v(x, y)$, and the subscripts indicate the appropriate derivatives. In case of ignoring y – dimension, the RDS system is modified to the resonant nonlinear Schrödinger equation as,

$$u_t^\alpha + \sigma^2 u_{xx} - 2\sigma^2 \left(\frac{|u|_{xx}}{|u|} \right) u - \omega |u|^2 u = 0$$

First of all, the (2 + 1)-dimensional imaginary Davey–Stewartson equations are converted into a system of NLODE to study and analyze its exact solutions.

Assuming the wave transformation, as

$$u(x, y, t) = e^i U(\xi), v(x, y, t) = V(\xi) \\ \xi = \mu \left(x + y - \frac{\eta t^\alpha}{\Gamma(\alpha + 1)} \right), \theta = \omega x + \beta y + \frac{\gamma t^\alpha}{\Gamma(\alpha + 1)} \tag{22}$$

Now applying Equation (22) on the (2 + 1)-dimensional Davey–Stewartson Equations (20) and (21), the following systems are obtained:

$$\mu^2 (1 - \sigma^2 - 2\sigma^4) U'' + \mu (\eta - 2\omega\sigma^2 - 2\beta) U - UV + \omega U^3 = 0 \tag{23}$$

$$\mu (\eta - 2\omega\sigma^2 - 2\lambda) i U' = 0 \tag{24}$$

$$-\mu^2 (1 - \sigma^2) V'' + 4\alpha\mu^2 (UU'' + U'^2) = 0 \tag{25}$$

We get Equation (26) by integrating Equation (25) twice with respect to and equaling the integration constant to zero.

$$V = \frac{2\omega}{1 - \sigma^2} U^2 \tag{26}$$

If the Equation (24) is taken as

$$\eta = 2\omega\sigma^2 + 2\lambda \tag{27}$$

Equation (26) is substituted into Equation (23), we get

$$-\mu^2 (1 - \sigma^2) (1 - \sigma^2 - 2\sigma^4) U'' - (1 - \sigma^2) (\gamma + \alpha^2\sigma^2 + \beta^2) U - (1 + \sigma^2) U^3 = 0 \tag{28}$$

Using the balancing term formula between the terms U'' and U^3 , relationship between n and M is examined.

$$M = n + 1 \tag{29}$$

Family 1. When $n = 2$ and $M = 3$ are substituted into Equation (14), the following results are obtained:

$$U = a_0 + a_1 F + a_2 F^2 \tag{30}$$

$$U' = a_1 b F + a_1 d F^3 + 2a_2 b F^2 + 2a_2 F^4 \tag{31}$$

$$U'' = a_1 b^2 F + 4a_2 b^2 F^2 + 4a_1 b d F^3 + 12a_2 b d F^4 + 3a_1 d^2 F^5 + 8a_2 d^2 F^6 \tag{32}$$

where $a_2 \neq 0, b \neq 0, d \neq 0$. Equations ((30)–((32)) are put into equation to obtain a system of algebraic Equation (28). The following results were obtained by solving this system with Wolfram Mathematica.

Case 1. Suppose that

$$b \neq d, a_0 = -\frac{b\mu\sqrt{2-6\sigma^2+4\sigma^4}}{\sqrt{\omega}}, a_1 = 0, a_2 = -\frac{2d\mu\sqrt{2-6\sigma^2+4\sigma^4}}{\sqrt{\omega}}$$

$$\gamma = -\beta^2 + 2b^2\mu^2(-1 + \sigma^2 + 2\sigma^4) - \sigma^2\omega^2 \quad (33)$$

we obtain

$$u_1(x, y, t) = e^{i(y\beta + x\omega + \gamma t^\alpha / \Gamma(1+\alpha))} \left(-\frac{a_0}{\sqrt{\omega}} - a_1 \left(\left(-\frac{d}{b} + ce^{-2b\mu(x+y-t^\alpha(2\beta+2\sigma^2\omega)) / \Gamma(1+\alpha)} \right) \sqrt{\omega} \right)^{-1} \right) \quad (34)$$

$$v_1(x, y, t) = \frac{2 \left(b\mu\sqrt{2-6\sigma^2+4\sigma^4} / \sqrt{\omega} + 2d\mu\sqrt{2-6\sigma^2+4\sigma^4} / \left(-d/b + ce^{-2b\mu(x+y-t^\alpha(2\beta+2\sigma^2\omega)) / \Gamma(1+\alpha)} \right) \sqrt{\omega} \right)^2 \omega}{1 - \sigma^2} \quad (35)$$

Equations (34) and (35) represent dark solutions as seen in Figure 1.

Case 2. Suppose that

$$b \neq d, \gamma = -\beta^2 + \omega^2, \sigma = -i \quad (36)$$

we get

$$u_2(x, y, t) = e^{i(y\beta + x\omega + \gamma t^\alpha / \Gamma(1+\alpha))} \times \left(a_0 + \frac{a_2}{-d/b + ce^{-2b\mu(x+y-t^\alpha\eta) / \Gamma(1+\alpha)}} + \frac{a_1}{\sqrt{-d/b + ce^{-2b\mu(x+y-t^\alpha\eta) / \Gamma(1+\alpha)}}} \right) \quad (37)$$

$$v_2(x, y, t) = \left(a_0 + \frac{a_2}{-d/b + ce^{-2b\mu(x+y-t^\alpha\eta) / \Gamma(1+\alpha)}} + \frac{a_1}{\sqrt{-d/b + ce^{-2b\mu(x+y-t^\alpha\eta) / \Gamma(1+\alpha)}}} \right)^2 \omega \quad (38)$$

These solutions are kink solutions as shown in Figure 2.

Case 3. Suppose that $b \neq d$

$$a_0 = \frac{i\mu\sqrt{-1+2\sigma^2}\sqrt{-(-1+\sigma^2)(\beta^2+\gamma+\sigma^2\omega^2)}}{\sqrt{\mu^2(-1+\sigma^2+2\sigma^4)}\sqrt{\omega}}, a_1 = 0$$

$$b = \frac{\sqrt{\beta^2+\gamma+\sigma^2\omega^2}}{\sqrt{2}\sqrt{\mu^2(-1+\sigma^2+2\sigma^4)}}, d = -\frac{ia_2\sqrt{\omega}\sqrt{\beta^2+\gamma+\sigma^2\omega^2}}{2\mu\sqrt{-2+4\sigma^2}\sqrt{-(-1+\sigma^2)(\beta^2+\gamma+\sigma^2\omega^2)}} \quad (39)$$

we get

$$u_3(x, y, t) = e^{i(y\beta + x\omega + \gamma t^\alpha / \Gamma(1+\alpha))} \left(\frac{a_2}{-d/b + ce^{-2b\mu(x+y-t^\alpha\eta) / \Gamma(1+\alpha)}} + \frac{i\mu\sqrt{-1+2\sigma^2}\sqrt{(1-\sigma^2)(\beta^2+\gamma+\sigma^2\omega^2)}}{\sqrt{\mu^2(-1+\sigma^2+2\sigma^4)}\sqrt{\omega}} \right), \quad (40)$$

$$v_3(x, y, t) = \frac{2\omega \left(a_2 / -d/b + ce^{-2b\mu(x+y-t^\alpha\eta) / \Gamma(1+\alpha)} + i\mu\sqrt{-1+2\sigma^2}\sqrt{(1-\sigma^2)(\beta^2+\gamma+\sigma^2\omega^2)} / \sqrt{\mu^2(-1+\sigma^2+2\sigma^4)}\sqrt{\omega} \right)^2}{1 - \sigma^2} \quad (41)$$

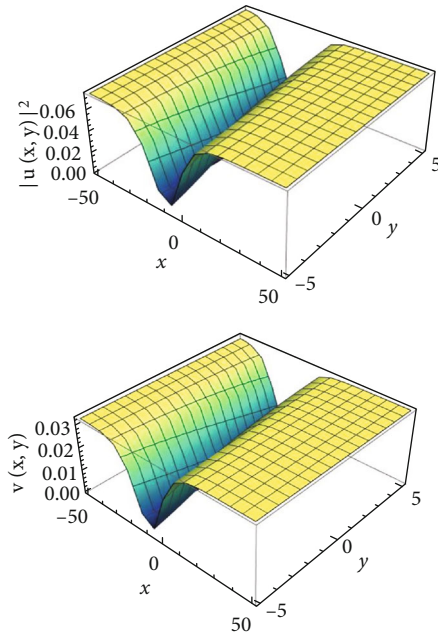


FIGURE 1: The 3-dimensional figures are drawn for solutions of Equations (34) and (35), when $c=0.1, b=1, d=-2, \mu=0.1, \eta=0.3, \omega=0.2, \beta=0.1, \alpha=0.2, \sigma=0.3, t=1/2$.

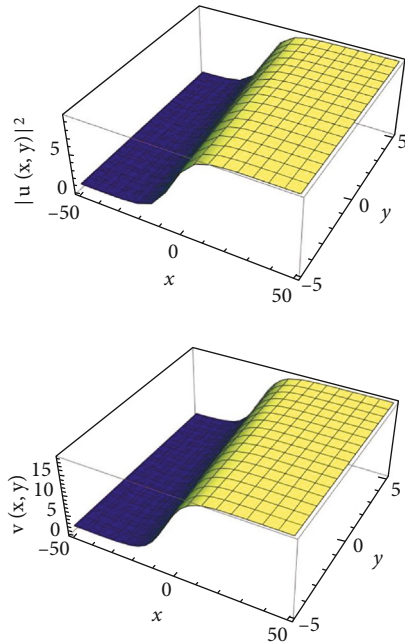


FIGURE 2: The 3-dimensional figures are drawn for solutions of Equations (37) and (38), when $a_0=1, a_1=0.1, a_2=2, c=0.2, b=1, d=-1, \mu=0.1, \omega=2, \beta=0.1, \alpha=0.2, \sigma=0.3, t=1/2$.

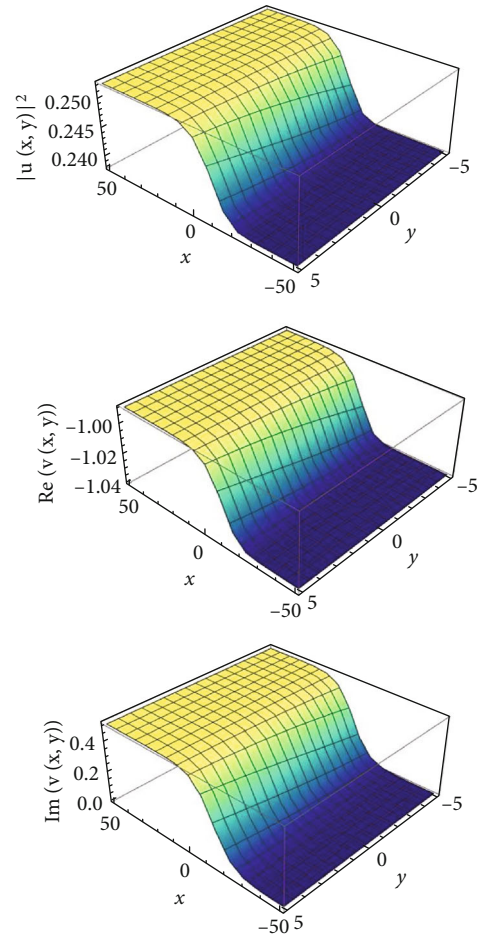


FIGURE 3: The 3-dimensional figures are drawn for solutions of Equations (40) and (41) when $a_2=0.12, c=0.2, b=1, d=-1, \mu=0.1, \omega=2, \beta=0.1, \gamma=0.2, \alpha=0.2, \sigma=0.3, t=1/2$.

These solutions are kink solutions as presented in Figure 3.

Case 4. Suppose that $b \neq d$.

$$a_0 = -\frac{\mu\sqrt{1-3\sigma^2+2\sigma^4}\sqrt{\beta^2+\gamma+\sigma^2\omega^2}}{\sqrt{\mu^2(-1+\sigma^2+2\sigma^4)}\sqrt{\omega}}, a_1 = 0$$

$$a_2 = -\frac{2d\mu\sqrt{2-6\sigma^2+4\sigma^4}}{\sqrt{\omega}}, b = \frac{\sqrt{\beta^2+\gamma+\sigma^2\omega^2}}{\sqrt{2}\sqrt{\mu^2(-1+\sigma^2+2\sigma^4)}} \tag{42}$$

we get

$$u_4(x, y, t) = e^{i(\gamma\beta+x\omega+t^\alpha\gamma/\Gamma(1+\alpha))} \left(-2d\mu\sqrt{2-6\sigma^2+4\sigma^4} \cdot \left(\left(-\frac{d}{b} + ce^{-2b\mu(x+y-\eta t^\alpha/\Gamma(1+\alpha))} \right) \sqrt{\omega} \right)^{-1} - a_0 \right) \tag{43}$$

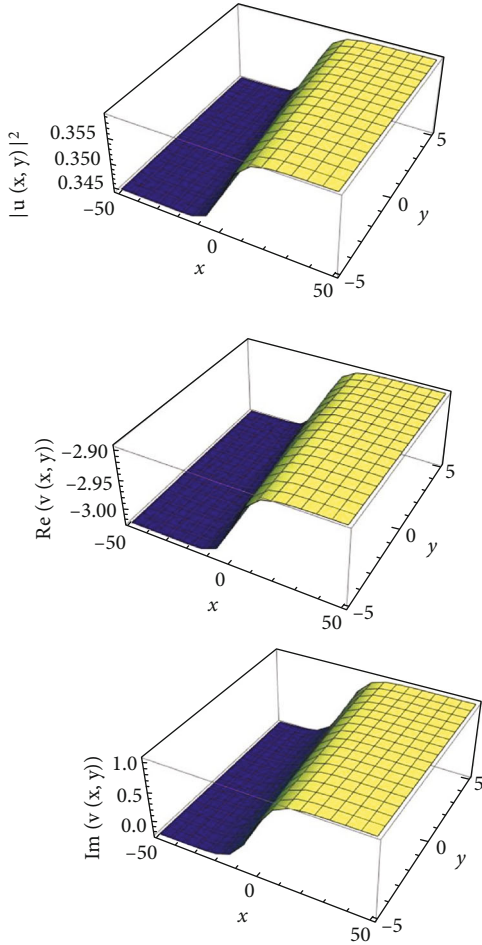


FIGURE 4: The 3-dimensional figures are drawn for solutions of Equation (43) and (44), when $a_2 = 0.12$; $c = 0.2$; $b = 1$; $d = -1$; $\mu = 0.1$; $\eta = 0.3$; $\omega = 4$; $\beta = 0.1$; $\gamma = 0.2$; $\alpha = 0.2$; $\sigma = 0.3$; $t = 1/2$.

$$v_4(x, y, t) = \frac{2\omega(-2d\mu\sqrt{2-6\sigma^2+4\sigma^4}((-d/b + ce^{-2b\mu(x+y-t^\alpha\eta/\Gamma(1+\alpha))})\sqrt{\omega})^{-1} - a_0)^2}{1-\sigma^2} \tag{44}$$

As shown in Figure 4, these solutions are kink solutions.

Case 5. Suppose that $b \neq d$.

$$a_1 = 0, b = \frac{a_0\sqrt{\omega}}{\sqrt{2}\sqrt{\mu^2(1-3\sigma^2+2\sigma^4)}}, d = \frac{a_2\sqrt{\omega}}{2\sqrt{2}\sqrt{\mu^2(1-3\sigma^2+2\sigma^4)}} \tag{45}$$

$$\gamma = -\beta^2 + \omega\left(\frac{a_0^2(1+\sigma^2)}{-1+\sigma^2} - \sigma^2\omega\right)$$

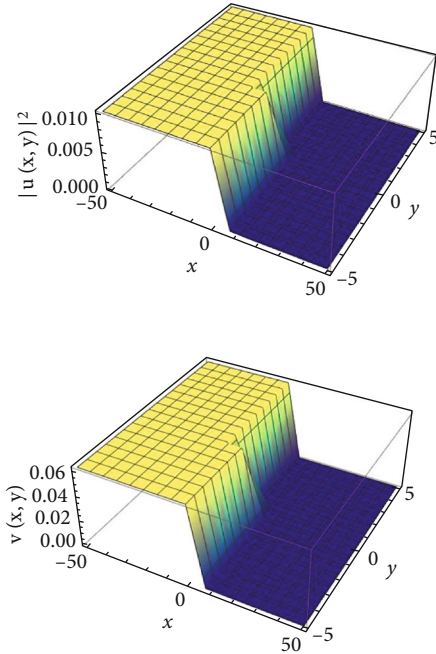


FIGURE 5: The 3-dimensional figures are drawn for solutions of Equations (46) and (47), when $a_0 = 0.1, a_2 = -0.2, c = 0.2, b = 1, d = -2, \mu = 6, \omega = 3, \beta = 2, \alpha = 0.2, \sigma = 0.2, t = 1/2$.

$$u_5(x, y, t) = e^{i(y\beta + x\omega + t^\alpha\gamma/\Gamma(1+\alpha))} \times \left(a_0 + a_2 \left(-\frac{d}{b} + ce^{-2b\mu(x+y-t^\alpha\eta/\Gamma(1+\alpha))} \right)^{-1} \right) \tag{46}$$

$$v_5(x, y, t) = \frac{2\left(a_0 + a_2\left(-d/b + ce^{-2b\mu(x+y-t^\alpha\eta/\Gamma(1+\alpha))}\right)^{-1}\right)^2 \omega}{1-\sigma^2} \tag{47}$$

As shown in Figure 5, these solutions are kink solutions.

Case 6. Suppose that $b \neq d$.

$$a_0 = \frac{b\mu\sqrt{2-6\sigma^2+4\sigma^4}}{\sqrt{\omega}}, a_1 = 0, a_2 = \frac{2d\mu\sqrt{2-6\sigma^2+4\sigma^4}}{\sqrt{\omega}}, \tag{48}$$

$$\gamma = -\beta^2 + 2b^2\mu^2(-1+\sigma^2+2\sigma^4) - \sigma^2\omega^2$$

we get

$$u_6(x, y, t) = e^{i(y\beta + x\omega + t^\alpha\gamma/\Gamma(1+\alpha))} \left(\frac{b\mu\sqrt{2-6\sigma^2+4\sigma^4}}{\sqrt{\omega}} + 2d\mu\sqrt{2-6\sigma^2+4\sigma^4} \cdot \left(\left(-\frac{d}{b} + ce^{-2b\mu(x+y-t^\alpha\eta/\Gamma(1+\alpha))} \right) \sqrt{\omega} \right) \right) \tag{49}$$

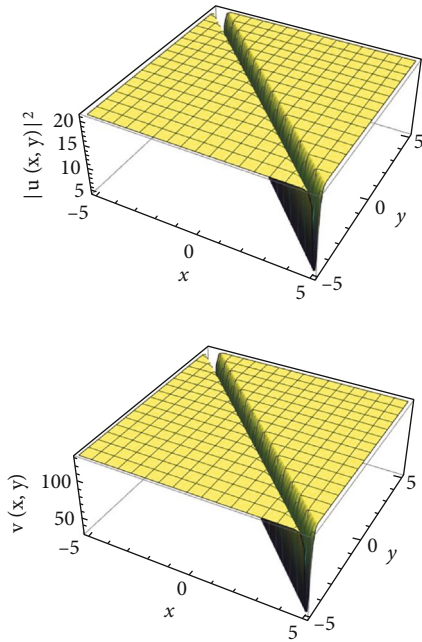


FIGURE 6: The 3-dimensional figures are drawn for solutions of Equations (49) and (50), when $a_0 = 0.1, a_2 = -0.2, c = 0.2, b = 1, d = -2, \mu = 6, \eta = 0.3, \omega = 3, \beta = 2, \alpha = 0.2, \sigma = 0.2, t = 1/2$.

$$v_6(x, y, t) = \frac{2(b\mu\sqrt{2-6\sigma^2+4\sigma^4}/\sqrt{\omega} + 2d\mu\sqrt{2-6\sigma^2+4\sigma^4}/(-d/b + ce^{-2b\mu(x+y-t^\alpha\eta/\Gamma(1+\alpha))})\sqrt{\omega})^2\omega}{1-\sigma^2} \quad (50)$$

As shown in Figure 6, solutions presented by Equations (49) and (50) are dark solutions.

Case 7. Suppose that $b \neq d$.

$$a_0 = \frac{\sqrt{\mu^2(1-3\sigma^2+2\sigma^4)}\sqrt{\beta^2+\gamma+\sigma^2\omega^2}}{\sqrt{\mu^2(-1+\sigma^2+2\sigma^4)}\sqrt{\omega}}, a_1 = 0, b = -\frac{\sqrt{\beta^2+\gamma+\sigma^2\omega^2}}{\sqrt{2}\sqrt{\mu^2(-1+\sigma^2+2\sigma^4)}} \\ d = -\frac{a_2\sqrt{\omega}}{2\sqrt{2}\sqrt{\mu^2(1-3\sigma^2+2\sigma^4)}} \quad (51)$$

we get

$$u_7(x, y, t) = e^{i(\gamma\beta+x\omega+t^\alpha\eta/\Gamma(1+\alpha))} \left(\frac{a_2}{-d/b + ce^{-2b\mu(x+y-t^\alpha\eta/\Gamma(1+\alpha))}} + a_0 \right) \quad (52)$$

$$v_7(x, y, t) = \frac{2\omega \left(a_2 (-d/b + ce^{-2b\mu(x+y-t^\alpha\eta/\Gamma(1+\alpha))})^{-1} + a_0 \right)^2}{1-\sigma^2} \quad (53)$$

As shown in Figure 7, solutions presented by Equations (52) and (53) are kink solutions.

5. Conclusion

In this investigation, we have studied that in the Resonant DS, equation plays a significant role in the dynamics and stability of fluid movement which in hydrodynamics, surface

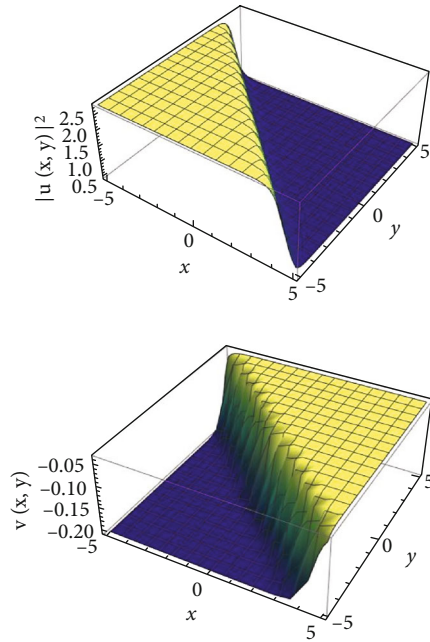


FIGURE 7: The 3-dimensional figures are drawn for solutions of Equations (52) and (53), when $a_2 = -2, c = 0.1, b = 1, d = -2, \mu = 2, \omega = 0.3, \beta = 0.2, \gamma = 0.2, \alpha = 0.2, \sigma = 3, t = 1/2$.

tension, and other capillary effects. We obtained exponential and complex wave solutions by applying the BSE method to (2 + 1)-dimensional time-fractional resonant Davey–Stewartson system equation. We have expressed by examining the structural parts of these exponential and complex solutions. Using this BSE method gives kink solutions for Equations (37) and (38), Equations (40) and (41), Equations (43) and (44), Equations (46) and (47), and Equation (52) and (53). The dark solution part is given by the Equation ((34)-(35)) and Equation ((49)-(50)). The graphs drawn in the article were re-examined by changing the values taken in the Mathematica program and the solutions were obtained in the same way as the kink-soliton and dark solution graphs. When we changed the given values in the Mathematica program, it gave a kink-soliton solution again. Three-dimensional surface graphics are drawn and supported separately for the real and imaginary parts of all solutions obtained.

6. Discussion

In this study, we use the Bernoulli subequation technique (BS-EM) to study a system, the (2 + 1)-dimensional resonant Davey–Stewartson. For this, we compare the solutions found using the usual (2 + 1)-dimensional resonant Davey–Stewartson system in the prior work with the solutions produced using the BS-EM. Comparing our answers leads us to the conclusion that they are distinct and more general. It provides many solutions when using the BS-EM. Depending on the coefficient values taken, the new solutions are different from those presented in the literature. In case of choosing $b \neq d, a_0 = -b\mu\sqrt{2-6\sigma^2+4\sigma^4}/\sqrt{\omega}, a_1 = 0, a_2 = -2d\mu\sqrt{2-6\sigma^2+4\sigma^4}$

$1/\sqrt{\omega}, \gamma = -\beta^2 + 2b^2\mu^2(-1 + \sigma^2 + 2\sigma^4) - \sigma^2\omega^2$, value in the system, different kink-soliton solutions emerge. It is possible to see that every answer that was found was unique. Additionally, as shown in Figures 1, 2, 3, 4, 5, 6, and 7, we provide 3D surface profiles and counterplots to help visualize the Resonant DS equation of certain derived solutions. After analysis, it was shown that the constraints that ensure the existence of soliton and kink solutions are connected to the coefficients $\omega, \beta, \gamma, \eta$.

Data Availability Statement

Data sharing is not applicable to this article as no new data were created or analyzed in this study.

Ethics Statement

Ethical approval is not applicable, because this article does not contain any studies with human or animal subjects.

Conflicts of Interest

The authors declare no conflicts of interest.

Author Contributions

Esin İlhan: conceptualization, methodology investigation, and editing. **Muhammed Yiğider:** conceptualization, methodology investigation. **Ercan Çelik:** visualization, supervision, editing. **Hasan Bulut:** writing–original draft preparation and editing. All authors read and approved the final manuscript.

Funding

No funding was received for this manuscript.

References

- [1] H. Rezazadeh, D. Kumar, A. Neirameh, M. Eslami, and M. Mirzazadeh, “Applications of three methods for obtaining optical soliton solutions for the Lakshmanan–Porsezian–Daniel model with Kerr law nonlinearity,” *Pramana*, vol. 94, no. 1, 2020.
- [2] T. A. Sulaiman, H. Bulut, G. Yel, and S. S. Atas, “Optical solitons to the fractional perturbed Radhakrishnan–Kundu–Lakshmanan model,” *Optical and Quantum Electronics*, vol. 50, no. 10, 2018.
- [3] H. F. Ismael and H. Bulut, “Nonlinear dynamics of (2+1)-dimensional Bogoyavlenskii Schieff equation arising in plasma physics,” *Mathematical Methods in the Applied Sciences*, vol. 44, no. 13, pp. 10321–10330, 2021.
- [4] H. F. Ismael, H. M. Baskonus, and H. Bulut, “Abundant novel solutions of the conformable Lakshmanan–Porsezian–Daniel model,” *Discrete and Continuous Dynamical Systems-S*, vol. 14, no. 7, pp. 2311–2333, 2021.
- [5] J. Manafian, O. A. İlhan, K. K. Ali, and S. Abid, “Cross-kink wave solutions and semi-inverse variational method for (3+1)-dimensional potential-YTSE equation,” *East Asian Journal on Applied Mathematics*, vol. 10, no. 3, pp. 549–565, 2020.
- [6] T. Yazgan, E. İlhan, E. Çelik, and H. Bulut, “On the new hyperbolic wave solutions to Wu-Zhang system models,” *Optical and Quantum Electronics*, vol. 54, no. 5, p. 298, 2022.
- [7] S. Ş. Kiliç and E. Çelik, “Complex solutions to the higher-order nonlinear Boussinesq type wave equation transform,” *Ricerche di Matematica*, vol. 73, no. 4, pp. 1793–1800, 2024.
- [8] J. Manafian, O. A. İlhan, H. F. Ismael, S. A. Mohammed, and S. Mazanova, “Periodic wave solutions and stability analysis for the (3+1)-D potential-YTSE equation arising in fluid mechanics,” *International Journal of Computer Mathematics*, vol. 98, no. 8, pp. 1594–1616, 2021.
- [9] W. X. Ma, T. Huang, and Y. Zhang, “A multiple exp-function method for nonlinear differential equations and its application,” *Physica Scripta*, vol. 82, no. 6, Article ID 065003, 2010.
- [10] P. Wan, J. Manafian, H. F. Ismael, and S. A. Mohammed, “Investigating one-, two-, and triple-wave solutions via multiple exp-function method arising in engineering sciences,” *Advances in Mathematical Physics*, vol. 2020, Article ID 8018064, 18 pages, 2020.
- [11] M. S. Osman and B. Ghanbari, “New optical solitary wave solutions of Fokas–Lenells equation in presence of perturbation terms by a novel approach,” *Optik*, vol. 175, pp. 328–333, 2018.
- [12] K. K. Ali, H. Dutta, R. Yilmazer, and S. Noeiaghdam, “On the new wave behaviors of the Gilson–Pickering equation,” *Frontiers in Physics*, vol. 8, no. 54, 2020.
- [13] H. F. Ismael, H. Bulut, H. M. Baskonus, and W. Gao, “Newly modified method and its application to the coupled boussinesq equation in ocean engineering with its linear stability analysis,” *Communications in Theoretical Physics*, vol. 72, no. 11, Article ID 115002, 2020.
- [14] A. Yokus, H. Durur, H. Ahmad, P. Thounthong, and Y. F. Zhang, “Construction of exact traveling wave solutions of the Bogoyavlenskii equation by $(G'/G, 1/G)$ -expansion and $(1/G')$ -expansion techniques,” *Results in Physics*, vol. 19, Article ID 103409, 2020.
- [15] H. Dutta, H. Günerhan, K. K. Ali, and R. Yilmazer, “Exact soliton solutions to the cubic-quartic non-linear Schrödinger equation with conformable derivative,” *Frontiers in Physics*, vol. 8, p. 62, 2020.
- [16] X. H. Zhao, B. Tian, X. Y. Xie, X. Y. Wu, Y. Sun, and Y. J. Guo, “Solitons, Bäcklund transformation and lax pair for a (2+1)-dimensional Davey–Stewartson system on surface waves of finite depth,” *Waves in Random and Complex Media*, vol. 28, no. 2, pp. 356–366, 2018.
- [17] X. Y. Tang, K. W. Chow, and C. Rogers, “Propagating wave patterns for the ‘resonant’ Davey–Stewartson system,” *Chaos, Solitons & Fractals*, vol. 42, no. 5, pp. 2707–2712, 2009.
- [18] N. Raza, S. Arshed, M. Bayram et al., “Exploration of novel solitary waves in presence of higher order polynomial nonlinearity and spatio-temporal dispersion via Itô calculus,” *Alexandria Engineering Journal*, vol. 114, pp. 179–197, 2025.
- [19] F. Javed, B. Rani, Y. Chahlaoui, H. M. Baskonus, and N. Raza, “Nonlinear dynamics of wave structures for the Davey–Stewartson system: a truncated Painlevé approach,” *Nonlinear Dynamics*, vol. 112, no. 24, pp. 22189–22200, 2024.
- [20] M. Eslami, M. Mirzazadeh, B. F. Vajargah, and A. Biswas, “Optical solitons for the resonant nonlinear Schrödinger’s equation with time-dependent coefficients by the first integral method,” *Optik*, vol. 125, no. 13, pp. 3107–3116, 2019.
- [21] G. Yuan and T. Xiao-Yan, “Symmetry analysis and similarity solutions of a resonant Davey–Stewartson system,” *Communications in Theoretical Physics*, vol. 52, no. 4, pp. 581–587, 2009.

- [22] Z. F. Liang and X. Y. Tang, “Painlevé analysis and exact solutions of the resonant Davey–Stewartson system,” *Physics Letters A*, vol. 374, no. 2, pp. 110–115, 2009.
- [23] X. R. Hu, Y. Chen, and L. J. Qian, “Full symmetry groups and similar reductions of a (2+1)-dimensional resonant Davey–Stewartson system,” *Communications in Theoretical Physics*, vol. 55, no. 5, pp. 737–742, 2011.
- [24] H. F. Ismael, S. S. Atas, H. Bulut, and M. S. Osman, “Analytical solutions to the M-derivative resonant Davey–Stewartson equations,” *Modern Physics Letters B*, vol. 35, no. 30, Article ID 2150455, 2021.
- [25] R. Khalil, M. Al Horani, A. Yousef, and M. Sababheh, “A new definition of fractional derivative,” *Journal of Computational and Applied Mathematics*, vol. 264, pp. 65–70, 2014.
- [26] D. Anker and N. C. Freeman, “On the soliton solutions of the Davey–Stewartson equation for long waves. Proceedings of the Royal Society of London,” *Proceedings of the Royal Society of London. A. Mathematical and Physical Sciences*, vol. 360, no. 1703, pp. 529–540, 1978.
- [27] E. Ilhan, *Some New Soliton Solutions of Time Fractional Resonant Davey–Stewartson Equations*, Authorea, 2021.